

Radical Product Yields from the Ozonolysis of Short Chain Alkenes under Atmospheric Boundary Layer Conditions

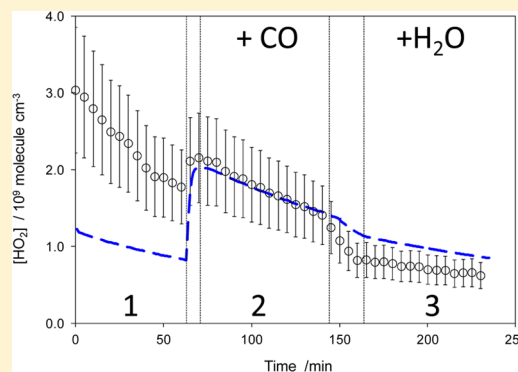
Mohammed S. Alam,[†] Andrew R. Rickard,^{‡,||} Marie Camredon,^{†,⊥} Kevin P. Wyche,^{§,#} Timo Carr,[§] Karen E. Hornsby,^{§,○} Paul S. Monks,[§] and William J. Bloss^{*,†}

[†]School of Geography, Earth & Environmental Sciences, University of Birmingham, Edgbaston, Birmingham B15 2TT, U.K.

[‡]School of Chemistry, University of Leeds, Leeds LS2 9JT, U.K.

[§]Department of Chemistry, University of Leicester, Leicester LE1 7RH, U.K.

ABSTRACT: The gas-phase reaction of ozone with unsaturated volatile organic compounds (VOCs), alkenes, is an important source of the critical atmospheric oxidant OH, especially at night when other photolytic radical initiation routes cannot occur. Alkene ozonolysis is also known to directly form HO₂ radicals, which may be readily converted to OH through reaction with NO, but whose formation is poorly understood. We report a study of the radical (OH, HO₂, and RO₂) production from a series of small alkenes (propene, 1-butene, *cis*-2-butene, *trans*-2-butene, 2-methylpropene, 2,3-dimethyl-2-butene (tetramethyl ethene, TME), and isoprene). Experiments were performed in the European Photoreactor (EUPHORE) atmospheric simulation chamber, with OH and HO₂ levels directly measured by laser-induced fluorescence (LIF) and HO₂ + ΣRO₂ levels measured by peroxy-radical chemical amplification (PERCA). OH yields were found to be in good agreement with the majority of previous studies performed under comparable conditions (atmospheric pressure, long time scales) using tracer and scavenger approaches. HO₂ yields ranged from 4% (*trans*-2-butene) to 34% (2-methylpropene), lower than previous experimental determinations. Increasing humidity further reduced the HO₂ yields obtained, by typically 50% for an RH increase from 0.5 to 30%, suggesting that HO_x production from alkene ozonolysis may be lower than current models suggest under (humid) ambient atmospheric boundary layer conditions. The mechanistic origin of the OH and HO₂ production observed is discussed in the context of previous experimental and theoretical studies.



1. INTRODUCTION

Alkenes, unsaturated hydrocarbons, are emitted to the atmosphere from a range of natural and anthropogenic sources, notably biogenic emissions of isoprene, C₅H₈, and the isoprenoid terpenes (C₁₀H₁₆) and sesquiterpenes (C₁₅H₂₄). Alkenes can contribute up to 30% of the total OH sink in urban regions,¹ and a higher proportion in forested environments;² atmospheric degradation of alkenes contributes to the production of ozone in the presence of nitrogen oxides and leads to the production of multifunctional oxygenated degradation products,³ which may act as precursors to, or contribute to the formation of, secondary organic aerosol (SOA).

In addition to degradation driven by reaction with OH and NO₃, alkene oxidation may be initiated by reaction with ozone, a process that leads to the nonphotolytic production of HO_x radical intermediates; detailed analyses of measurements from atmospheric field campaigns have shown ozonolysis to account for up to 30% of the total OH radical production.⁴ Understanding the yields of OH, HO₂, and RO₂ radicals and their dependence upon atmospheric conditions is essential to quantify this important contribution to atmospheric oxidizing capacity.

Gas-phase alkene ozonolysis is believed to proceed via the Criegee mechanism,⁵ illustrated in Figure 1. Ozonolysis is highly exothermic, initiated by the electrophilic cycloaddition of ozone across the C=C double bond to form an unstable 1,2,3 trioxolane (hereafter referred to as a primary ozonide, POZ) (R1). This intermediate is high in energy and rapidly decomposes at the central C–C bond and one of the O–O bonds. Given that the O–O bond can break at two different sites, two alternative pairs of carbonyl oxides (hereafter referred to as Criegee intermediates, CIs) and stable carbonyl molecules can be formed (R2a and R2b).

The CI and carbonyl coproduct produced from the exothermic decomposition of the POZ possess a significant amount of vibrational excitation. This energy enables further unimolecular reactions of the excited CI to occur but is not sufficient for the decomposition of the carbonyl molecule;¹ Figure 2. The distribution of decomposition products of the POZ is dependent upon the chemical conditions and substitution of the alkene. Different CIs behave as distinct

Received: September 1, 2013

Revised: October 29, 2013

Published: October 30, 2013

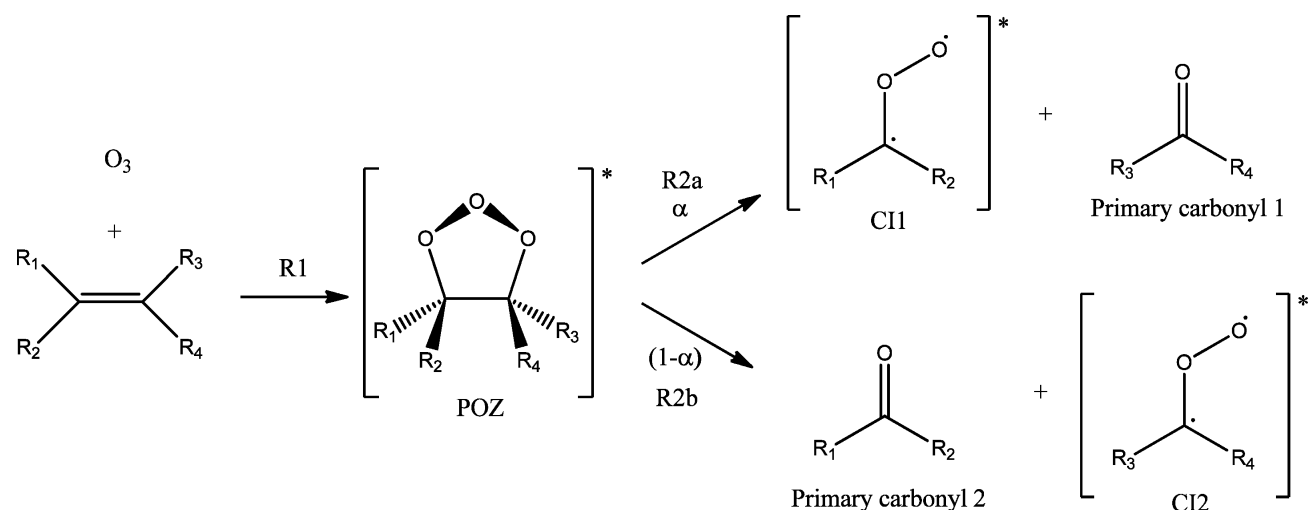


Figure 1. Cycloaddition of ozone across the alkene double bond and subsequent decomposition of the POZ: the Criegee mechanism.

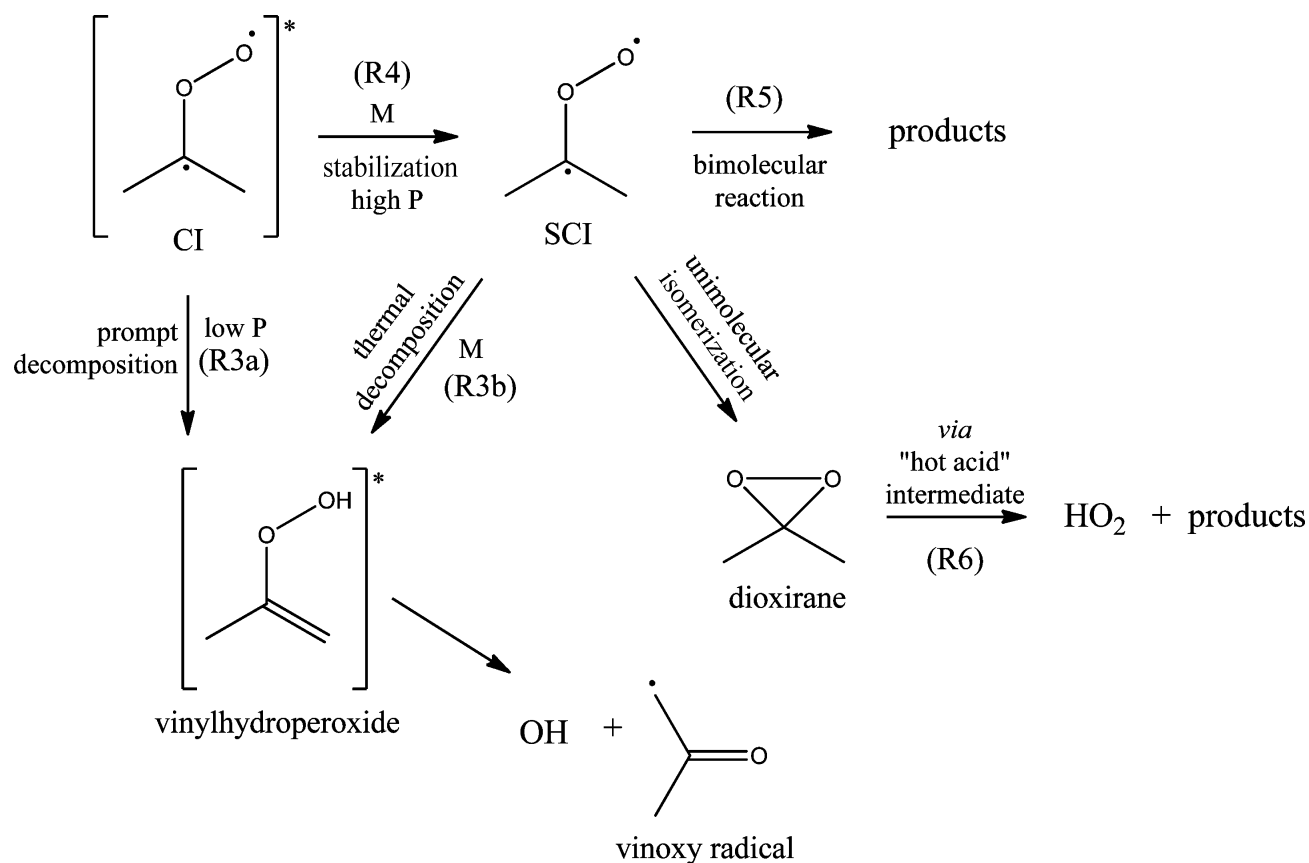


Figure 2. Potential fates of the Criegee intermediate.

chemical entities as demonstrated by the range of detected experimental products, dependent upon the extent of the substitution of the CI and distribution of energy following decomposition of the POZ.³ Substituted CIs can be formed in a *syn* (i.e., with the alkyl substituent on the same side of the CI as the terminal O atom) configuration or *anti* configuration, with a substantial barrier to interconversion between the two.⁶

Briefly, *syn*- and disubstituted CIs are thought to predominantly decompose through isomerization via a five-membered transition state to give an excited vinyl hydroperoxide intermediate, which subsequently decomposes to give

OH and a vinyloxy radical (R3a; the hydroperoxide mechanism).³ The proportion of the vibrationally excited CIs that have insufficient energy to isomerize/decompose may form so-called stable Criegee intermediates (SCIs), either directly following decomposition of the primary ozonide or through collisional stabilization of the CI (R4), which can subsequently undergo bimolecular reactions⁷ or decomposition (leading to further, delayed production of OH, again via a vinyl hydroperoxide intermediate (R3b), or potentially to HO₂, via a dioxirane/hot acid intermediate (R6)). The prevailing conditions (pressure; experimental time scale) have been

shown to be critical in controlling the observed formation of OH, SCIs, and other products.⁸

The vinoxy radical formed alongside OH (Figure 2) will react with oxygen in the atmosphere to form an excited β -oxo peroxy radical, which may be stabilized or undergo decomposition forming CO, a (secondary) stable carbonyl species and OH.⁹ However, this pathway to OH formation is only thought to be significant if an aldehydic hydrogen is present.³ The stabilized β -oxo peroxy radical may then undergo self- or cross-reaction with other peroxy radicals to form stable species such as glyoxal, methylglyoxal, glycolaldehyde, peroxides, and further secondary carbonyls.

The fate of the *anti*-CI and of the CH₂OO CI formed from terminal alkenes differs in that the hydroperoxide rearrangement is not available. Briefly, the *anti*-CI (and CH₂OO) can undergo rearrangement through a dioxirane structure, which can decompose to various products including OH, HO₂, CO, CO₂, H₂O, and alkyl molecules via a hot acid/ester intermediate.¹ The *syn*- and *anti*-CIs can also undergo stabilization followed by bimolecular reaction, but studies suggest that stabilization is a minor process for disubstituted and *syn*-monosubstituted CIs, as their lifetime with respect to the vinyl hydroperoxide mechanism is thought to be substantially shorter than the time required for bimolecular processes to occur,^{10,11} although recent experiments have shown that the vinyl hydroperoxide intermediate itself may have an appreciable lifetime.^{8,12} Collisional stabilization (or possible direct formation) of SCIs may be followed by a range of bimolecular reactions with atmospherically relevant species such as H₂O, NO₂, SO₂, and CO,^{1,13,14} alongside thermal decomposition. Very recent results indicate that reactions of the SCIs with SO₂ and NO₂ proceed much faster than previously thought and that the reaction with water is comparatively slow, suggesting an important role for SCIs as atmospheric oxidants.^{15–17}

Laboratory Measurements of HO_x Radical Production from Alkene Ozonolysis. The first indications for the production of radical species, including OH, from gas-phase alkene ozonolysis reactions arose through observations of chemiluminescence, attributed to emission from vibrationally and electronically excited OH, observed at low pressures (1–10 Torr) from the reaction between ozone and a range of short chain alkenes (C₂–C₆);¹⁸ the observed OH was attributed to the decomposition of an excited Criegee intermediate, generating H atoms that would rapidly be converted to OH radicals via reaction with O₃.^{19,20} Direct formation of OH through ozonolysis reactions at atmospheric pressure via a vinyl hydroperoxide channel was first proposed for 2,3-dimethyl-2-butene by Niki et al.,⁷ who measured the reaction stoichiometry of $\Delta[2,3\text{-dimethyl-2-butene}]/\Delta[\text{O}_3]$ to derive an OH radical yield of 0.70 ± 0.10 .

A number of studies have followed, reporting quantitative indirect and direct OH yield measurements for the ozonolysis of various alkenes, using one of three generalized approaches: (i) indirect measurements, where a radical scavenger or tracer(s), reactive toward OH but not toward O₃ or other reactants, are used to infer the cumulative OH production in the system at long (minutes +) time scales;^{21–24} (ii) direct observations using techniques such as laser-induced fluorescence (LIF),²⁵ peroxy radical chemical amplification (PERCA),²⁶ or matrix isolation–electron spin resonance (MIERS)²⁷ are used to quantify HO_x radicals under steady-state conditions or (in laboratory settings) at short reaction

times; or (iii) turnover experiments in which the additional removal of the alkene (due to reaction with OH) or ozone (due primarily to reaction with HO₂) is used to infer OH and/or HO₂ production, again at long (minutes +) time scales.²⁸

The majority of OH radical yields reported have been obtained through tracer^{21,22} and scavenger methods.^{23,24} In some cases these approaches can be problematic, for example, with the cyclohexane scavenger approach, production of the observed products (usually cyclohexanol and/or cyclohexanone) depends upon the radical population actually present (through dependencies upon RO₂ vs. HO₂ competition for the cyclohexylperoxy radical) and hence can vary significantly between chemical systems and within the same system as the chemical composition evolves.²⁹ Other OH scavenger techniques have included the use of excess 2-butanol³⁰ and CO,³¹ monitoring the reaction products 2-butanone and CO₂, respectively. Yields of OH from alkene-ozone reactions have also been derived by adding relatively small quantities of tracer compounds (e.g., 1,3,5-trimethylbenzene, *m*-xylene, and di-*n*-butyl ether) to scavenge OH radicals. Such tracers exhibit varying reactivity to OH, allowing the determination of OH yields in an ozonolysis system by comparing the relative decay ratios of tracer pairs, through knowledge of their OH reaction rate coefficients.²¹ Indirect OH yield measurements using both the scavenger and tracer techniques agree reasonably well, and an extensive, generally self-consistent database now exists.^{1,3}

The first direct observation of OH production from alkene ozonolysis was obtained by Donahue et al.,²⁵ who employed LIF to monitor OH production from a range of small alkenes at low pressure (4–6 Torr). In subsequent work,^{32–34} OH yields were found to be pressure-dependent for substituted alkenes, with fast OH formation (time scales of a few ms) effectively quenched as pressures approach ca. 400 Torr; however, on long time scales (ca. 1 s), the OH yield increased, approaching values consistent with other longer-time scale atmospheric pressure measurements from radical scavenger/tracer experiments, indicating that the majority of the observed OH for substituted alkenes under tropospheric conditions arises from the decomposition of thermalized carbonyl oxides and/or vinyl hydroperoxides, with a contribution from prompt decomposition (although the latter will dominate for ethene and the CH₂OO Criegee intermediate formed from terminal alkenes).⁸ These results indicated that OH formation from alkene ozonolysis can result from both prompt formation, from a vibrationally excited CI, and from the decomposition of a partially stabilized CI on longer time scales,³ therefore opening the possibility for bimolecular reactions to occur with the SCI, interrupting the decomposition process and reducing the OH yields. This possibility has been investigated for various SCI scavengers, including H₂O, SO₂, butanone, and acetic acid for 2-methyl-2-butene;¹⁴ CH₃CHO for *trans*-2-butene;¹⁰ and NO₂ for 2,3-dimethyl-2-butene, *trans*-5-decene, cyclohexene, and α -pinene,³⁵ with little reduction in (inferred) OH yield found, indicating that production of OH through the unimolecular decomposition of partially stabilized CIs is significantly larger than the rate of reaction with the potential SCI scavengers studied, at least for those species and experimental conditions employed. Subsequent direct measurements of steady-state OH abundance and hence overall production, using LIF systems incorporated within simulation chambers, have been reported for 2,3-dimethyl-2-butene, 2-methyl-2-butene, *trans*-2-butene, and α -pinene,³⁶ for isoprene,²⁴ and for ethene.²⁹ Overall, the substantial experimental database for OH yields on long

(seconds +) time scales relevant to the impact of ozonolysis reactions upon the atmosphere is broadly consistent across a range of direct and indirect approaches.

In contrast to the substantial body of experimental data on OH production, the observational database for direct HO₂ production from alkene ozonolysis is sparse and inconsistent; even more so for RO₂. In the absence of experimental data, some modeling studies have necessarily assumed a 1:1 stoichiometry for production of OH and a radical coproduct;³⁷ however, the existence of secondary channels for the production of OH⁹ and for the production of two HO₂ radicals from the CH₂OO CI formed from terminal alkenes^{1,29} indicate that this supposition may not hold. Mihelcic et al.²⁷ used the matrix isolation–electron spin resonance (MIESR) approach to measure the OH and HO₂ yields from ethene ozonolysis, obtaining yields of 20 ± 2 and 39 ± 3%, respectively. Radical production in the ethene–ozone system has also been investigated using a laboratory PERCA methodology combined with detailed modeling, to extract yields of HO₂ and HO₂ + RO₂ of 38 ± 2 and 45 ± 3%, respectively;²⁶ subsequently, this approach was extended to propene, with yields of 39 ± 8%, 19 ± 4%, and 39 ± 8% obtained for OH, HO₂, and CH₃O₂, respectively.³⁸ Radical yields have been deduced from experiments in the SAPHIR simulation chamber, in which the decay of the additional turnover of the alkene and/or ozone, in experiments performed with/without an OH scavenger (excess CO) were used to infer OH and HO₂ yields.²⁸ In contrast to previous tracer/scavenger studies, the OH yields obtained varied with humidity, increasing in the presence of H₂O, and the inferred (dry) HO₂ yields (propene, 1.50 ± 0.75; 1-butene, 1.60 ± 0.80; and isobutene, 2.00 ± 1.00) were substantially greater than those reported in the direct measurements (and assumed in most atmospheric mechanisms). Most recently, the LIF/chemical conversion technique was used to determine an HO₂ yield of 0.26 ± 0.03 for isoprene ozonolysis in a small simulation chamber.²⁴

The existing experimental data set is therefore in reasonable agreement with regard to OH production (yields) from alkene ozonolysis, which are broadly consistent with the dominant OH production channel for substituted alkenes being the hydroperoxide mechanism for the *syn*-CI, with additional OH production potentially arising from further decomposition of the coformed alkoxy radical and from decomposition of the *anti*-CI conformer.³ In the case of terminal alkenes and ethene, decomposition of the C₁ CI, CH₂OO, also leads to direct OH production.²⁹ The mechanistic origin and yield of HO₂ is rather less clear; in the ethene system, HO₂ is produced through decomposition of the CH₂OO CI (potentially via a hot acid intermediate), while for substituted alkenes the literature observations of substantial HO₂ production noted above indicate that further decomposition of one or both CIs (in addition to OH production via the hydroperoxide mechanism) may occur. The experimental yields of HO₂ reported are substantially greater than the OH yields in the limited number of studies reported (e.g., ethene; ca. 40% for HO₂ compared with 10–20% for OH across a number of measurements), with substantial inconsistency apparent between studies; this may in part reflect the greater complexity of interpretation of HO₂ data in the presence of multiple chemical source and sink processes. As NO-driven RO₂–HO₂–OH radical cycling within the atmosphere is likely to be significant in most environments where the alkene abundance is substantial, characterizing non-OH radical production from alkene ozonolysis is of importance

for a quantitative understanding of atmospheric oxidation. Improved understanding is also necessary to address the potential for other atmospheric reactants, such as water vapor, to affect the OH (and in particular HO₂) radical yields. Atmospheric chemical mechanisms employ radical (HO₂, RO₂) yields, which are largely inferred through the observation of associated stable products on the basis of the mechanistic understanding outlined above³⁹ and, in the case of HO₂, are substantially lower than those suggested by some of the studies noted above.^{28,38} In this article, we present systematic measurements of radical yields from the ozonolysis of propene, 1-butene, 2-methylpropene, *cis*-2-butene, *trans*-2-butene, 2,3-dimethyl-2-butene, and isoprene, obtained through simulation chamber experiments performed in the EUPHORE (European Photoreactor) facility, and employing LIF and PERCA techniques to monitor OH (directly), HO₂, and RO₂ radicals.

2. APPROACH: EUPHORE CHAMBER EXPERIMENTS

Detailed accounts of EUPHORE, the monitoring techniques used and experimental procedure followed can be found elsewhere;^{40,41,29} a brief overview is provided here. The EUPHORE facility comprises two ca. 200 m³ reaction chambers, formed from FEP film, with housings that may be closed to exclude light. Chamber pressure is maintained ca. 100 Pa above ambient and chamber temperatures at near ambient levels (cooled through a chilled floor). For all the experiments described here, the chamber covers were closed, excluding ambient sunlight ($j(\text{NO}_2) < 2 \times 10^{-6} \text{ s}^{-1}$). The chambers are mixed by fans on a time scale of 3 min. The chamber is filled with scrubbed dry air, to which reactants of interest are added volumetrically by direct injection, and the evolving composition monitored as a function of time. Dilution (arising from sample withdrawal, as total chamber pressure is maintained by addition of scrubbed air) is monitored by following the decay of SF₆, added as a tracer prior to each experiment, and during the work described here typically corresponded to a first-order decay rate of ca. 10⁻⁵ s⁻¹, accounting for between 2 and 42% of the alkene removal across all experiments (values for 2,3-dimethyl-2-butene and propene, respectively; balance through chemical processes). Alkene and stable product concentrations were monitored by Fourier-transform infrared absorption spectroscopy (FTIR), and by chemical ionization reaction time-of-flight mass spectrometry (CIR-TOF-MS) in the case of oxygenated products. Levels of O₃ (UV photometry), NO_x (chemiluminescence with photolytic converter; below detection limit for all (dark, NO_x-free) experiments described here), and CO (infrared absorption) were followed by conventional monitors. Chamber humidity was measured using a chilled-mirror dew-point hygrometer. OH radicals were observed directly using laser induced fluorescence spectroscopy (LIF), while HO₂ radicals were detected following their titration to OH by added NO within the LIF instrument.^{36,42} The sum of hydro- and organic peroxy radicals, HO₂ + ΣRO₂, was measured using a peroxy radical chemical amplifier (PERCA).⁴³

Instrumental Accuracy. The results reported in this study were derived using a comprehensive suite of measurement instrumentation. Alkene and ozone concentrations were determined by FTIR and converted to mixing ratios through the measured chamber temperature and pressure. Systematic uncertainties arising from the literature cross-sections were conservatively estimated to be 10% (the FTIR O₃ data agreed very well with measurements made by UV photometry). The radical measurements were performed by LIF (OH and HO₂)

and PERCA ($\text{HO}_2 + \Sigma\text{RO}_2$). The LIF system was calibrated before, during, and after each measurement campaign using the H_2O photolysis/ozone actinometry approach,⁴⁴ and calibrations were constant to within a few percent. The estimated uncertainty in the LIF data from a single calibration is 27% (combined systematic error and precision)⁴² although this may be regarded as conservative as the precision component of this uncertainty within a single calibration will, to a certain extent, average out across the experiments. The instrument was calibrated as a function of humidity; in keeping with previous results⁴⁵ a reduction in the instrument sensitivity is observed as humidity increases compared with that measured under dry conditions, but the response flattens out (and was fully characterized) within the humidity range employed here. The potential for interference from substituted peroxy radicals in the LIF HO_2 measurement is considered explicitly in the analysis section below. The PERCA was calibrated using the photolysis of methyl iodide/air mixtures to form methylperoxy radicals, thus determining the chain length of the chemical amplification.⁴⁶ An NO_2 permeation device was used to determine the sensitivity of the Scintrex (Luminol chemiluminescence detector) to the NO_2 product of the amplification. The overall accuracy of the peroxy radical measurements was estimated to be 38% (2 SD) from the combined uncertainties associated with the radical calibration, NO_2 quantification, and humidity correction.⁴⁷

Experimental Procedure. All experiments were initiated in a clean (flushed overnight) dry chamber. Ozone (generated online by corona discharge) and (if necessary) water vapor and/or OH scavengers (CO or cyclohexane) were added to the required levels, followed by an aliquot of SF_6 (as a tracer for dilution). The ozonolysis reaction was initiated by injection of the relevant alkene using a graduated syringe, with reactant and product concentrations monitored over a time scale of 1–2 h, at a time resolution ranging from 1 min (LIF, PERCA) to 10 min (FTIR scan period), which may be compared with the chamber mixing time of 3 min. Three sets of experimental conditions were employed: (i) simple alkene–ozone only systems; (ii) experiments with added excess CO (ca. 500 ppm) as an OH scavenger, to suppress the OH + alkene reaction; and (iii) experiments performed with added water vapor (to 30% RH); the dry chamber humidity was approximately 0.3% (measured dew point -45 °C). The experimental conditions and chemical systems studied are summarized in Table 1.

3. APPROACH: DATA ANALYSIS

To account for secondary chemical processes (radical sinks and additional sources), the measurements were interpreted using a

Table 1. Range of Initial Conditions Used for EUPHORE Experiments^a

species	alkene (ppb)	O_3 (ppb)	H_2O range (RH %)
propene	300	300	0.3–30%
1-butene	300	300	0.3–30%
<i>cis</i> -2-butene	100	200	0.3%
<i>trans</i> -2-butene	100–200	100–200	0.3–30%
2-methylpropene	100–200	200–500	0.3–30%
2,3-dimethyl-2-butene	30–50	25–30	0.3%
isoprene	100–200	200–300	0.3%

^aAdditional reagents SF_6 (dilution tracer) and CO (OH scavenger) added for some experiments.

detailed chemical model, within which the yields of OH and HO_2 were optimized to match the observed data. The model reaction scheme was based upon the relevant subset of the Master Chemical Mechanism (MCM) version 3.2^{39,48} for the degradation of each alkene in question, including inorganic reactions and updated cyclohexane degradation chemistry as described in ref 29. Model conditions (temperature, pressure, and dilution rate) were set to the corresponding mean value for each experiment (as variability in these parameters was negligible during each run) and simulations initialized with the relevant experimental conditions as outlined in Table 1. Within the model, the actual ozonolysis process (i.e., Criegee decomposition reactions) were updated from the MCM representation to reflect a more detailed description of the actual mechanism: The primary ozonide (POZ) was assumed to decompose rapidly, and then each initially formed (excited) Criegee intermediate to further decompose to form radical products and stable species or to undergo collisional stabilization forming a stabilized Criegee intermediate (SCI), from which no further radical formation occurred. These reactions (2–6 in Figure 2) were not assigned individual rate constants, as the process occurred effectively instantaneously on the time scale of the experiments (of the order of minutes), but rather a branching ratio for each potential decomposition/stabilization product was used. This approach implicitly groups together CI, SCI, and vinyl hydroperoxide decomposition routes, irrespective of the differing time scales (microsecond vs millisecond) over which they may occur, as long as these are shorter than the experimental time scale (2–3 min, determined by the chamber mixing time). A consequence of this approach is that processes such as SCI thermal decomposition would be interpreted here as formation of the resulting decomposition products, rather than of SCIs, as long as such transformations occurred on a time scale of the order of tens of seconds or faster; this consideration must be noted when comparing the results obtained here to those reported from (e.g.) millisecond time scale laboratory measurements, considered further below. Similarly, the decomposition/ O_2 reaction converting HCO into $\text{HO}_2 + \text{CO}$ and H atoms into HO_2 were implicitly adopted, following the MCM protocol.³⁹ Rate constants for the subsequent bimolecular reactions of the SCI with CO and H_2O were taken directly from the MCM v3.2. The impact of recent measurements, suggesting some SCI reactions may be much faster than the values used within the MCM,¹⁵ is discussed later.

An iterative approach was adopted to derive the OH and HO_2 yields, to account for the interdependence between these quantities. It was not possible to derive both yields from a single experiment, due to interferences in the HO_2 measurement from substituted organic peroxy radicals, formed following the OH + alkene reaction, in the absence of an OH scavenger (see discussion below). Three stages were followed: (i) OH yields were optimized, using measured OH data obtained from experiments performed without an OH scavenger (Table 1). The HO_2 concentrations measured in these runs were found to include a substantial interference component from substituted peroxy radicals (measurements hereafter referred to as HO_2^* , see below) and were not used to constrain the optimization; rather HO_2 yields were fixed at MCM v3.2 values. (ii) HO_2 yields were obtained using measured HO_2 data obtained from experiments performed with an OH scavenger present (in which the interferant organic peroxy radicals are absent). Finally, (iii) the OH yields were

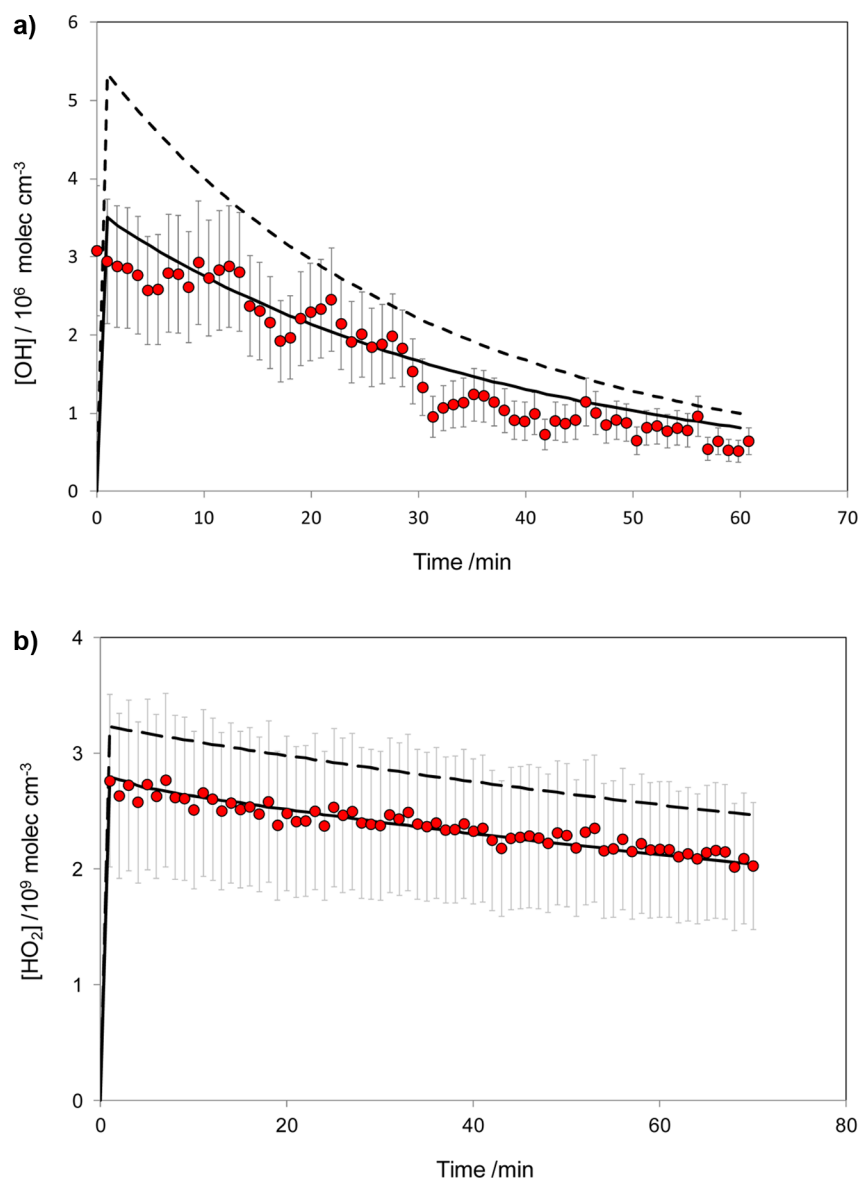


Figure 3. (a) Temporal profile of OH (red circles) plus model simulations before (dashed line, base case MCM v3.2 chemistry) and after (solid line) optimizing the OH yield to the LIF data (see Table 1), for *cis*-2-butene ozonolysis. (b) Equivalent plot for HO₂ measurements and model predictions (MCM v3.2 and following yield optimization) for 1-butene ozonolysis.

reoptimized, from nonscavenger experiments, using the actual HO₂ yields obtained in the second stage. Optimization was performed within the FACSIMILE solver.⁴⁹ In principle one could repeat the iteration to continue refinement; however, in practice, the change in OH yields resulting from this single repetition was <5% in all cases. Sensitivity analyses were performed to assess the cross-dependence of the OH and HO₂ yields obtained following this approach. For the worst case system considered (propene, slowest ozonolysis reaction rate, hence largest contribution from secondary HO₂/OH interconversion via reaction with O₃) varying the HO₂ channel yield from 0.08 (as shown for reaction R10d, below) to 0.77 (the upper limit possible considering observations of stable product channels R10b and R10c)⁵⁰ corresponded to a reduction in OH yield from 0.36 to 0.29, reflecting the relatively limited contribution of HO₂ + O₃ to OH production.

Within the modeled reaction scheme, the branching ratio between isomerization/decomposition of the *syn*-CI producing OH (via the hydroperoxide mechanism) and its potential

collisional stabilization was optimized in order to obtain an OH yield, taking into account any secondary OH formation through inclusion of the full degradation chemistry within the model. Decomposition yields for the most simple (C₁) CI, CH₂OO*, formed from all terminal alkenes, were fixed at the values determined by Alam et al.²⁹ Stable product yields for the substituted CIs were taken from the literature¹ and have minimal impact upon the derived radical yields under the conditions of these experiments. The ratio of the two CIs formed (i.e., the value of α) was determined from stable product yields;²⁹ the values used for propene, 1-butene, and 2-methylpropene were 51:49 for [CH₃CHOO]* + HCHO (R8a)/[CH₂OO]* + CH₃CHO (R8b), 59:41 for [C₂H₅CHOO]* + HCHO/[CH₂OO]* + CH₃CH₂CHO, and 34:66 for [CH₂OO]* + CH₃COCH₃/[(CH₃)₂COO]* + HCHO, respectively. In the cases of *cis*- and *trans*-2-butene, 50:50 yields of the relevant CIs were used.²² The optimization approach adopted to obtain HO₂ yields for each system studied was as follows. As noted above, degradation products of the

Table 2. OH Yields, All under Dry Conditions (RH < 0.4%) unless Noted

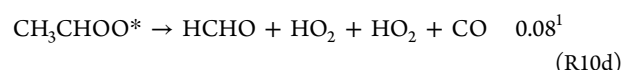
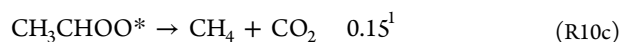
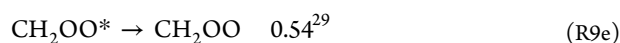
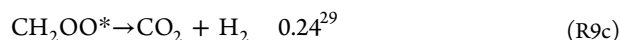
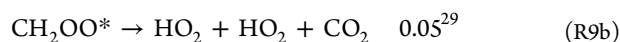
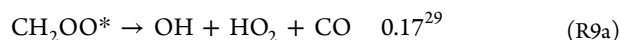
parent alkene; CIs formed	OH yield	method	ref
ethene	0.17 ± 0.09	LIF	Alam et al. ²⁹
CH ₂ OO	0.16		IUPAC ⁵⁰
	0.13		MCM ³⁹
propene	0.36 ± 0.10	LIF	this study
	0.34		IUPAC ⁵⁰
CH ₂ OO	0.36		MCM ³⁹
CH ₃ CHOO	0.33 (+0.17/−0.11)	cyclohexane	Atkinson & Aschmann ⁶⁸
	0.18 ± 0.01	CO	Gutbrod et al. ³¹
	0.34 ± 0.06	cyclohexane	Neeb & Moortgat ⁶⁹
	0.35 ± 0.07	tracer	Paulson et al. ²¹
	0.32 ± 0.08	tracer	Rickard et al. ²²
	0.40 ± 0.06	2,3-butandiol	Aschmann et al. ⁷⁰
	0.10 ± 0.07	stoichiometry	Wegener et al. ²⁸
	0.30 ± 0.08 (RH ≈ 32%)	stoichiometry	Wegener et al. ²⁸
	0.39 ± 0.08	PERCA	Qi et al. ³⁸
1-butene	0.56 ± 0.15	LIF	this study
	0.36		MCM ³⁹
CH ₂ OO	0.41 (+0.21/−0.14)	cyclohexane	Atkinson & Aschmann ⁶⁸
CH ₃ CH ₂ CHOO	0.29 ± 0.04	tracer	Paulson et al. ²¹
	0.26	tracer	Fenske et al. ¹⁰
	0.00 ± 0.08	stoichiometry	Wegener et al. ²⁸
	0.30 ± 0.09 (RH ≈ 32%)	stoichiometry	Wegener et al. ²⁸
2-methylpropene	0.67 ± 0.18	LIF	this study
	0.62		IUPAC ⁵⁰
CH ₂ OO	0.82		MCM ³⁹
(CH ₃) ₂ COO	0.84 (+0.42/−0.28)	cyclohexane	Atkinson & Aschmann ⁶⁸
	0.60 (+0.05/−0.07)	cyclohexane	Neeb & Moortgat ⁶⁹
	0.72 ± 0.12	tracer	Paulson et al. ²¹
	0.60 ± 0.15	tracer	Rickard et al. ²²
	0.30 ± 0.14	stoichiometry	Wegener et al. ²⁸
	0.80 ± 0.10 (RH ≈ 32%)		Wegener et al. ²⁸
cis-2-butene	0.26 ± 0.07	LIF	this study
	0.33		IUPAC ⁵⁰
CH ₃ CHOO	0.57		MCM ³⁹
	0.41 (+0.21/−0.14)	cyclohexane	Atkinson & Aschmann ⁶⁸
	0.14 ± 0.03	stoichiometry	Horie et al. ⁷¹
	0.17 ± 0.02	CO	Gutbrod et al. ³¹
	0.33 ± 0.07	tracer	McGill et al. ⁷²
	0.33 ± 0.05	tracer	Orzechowski & Paulson ⁷³
	0.18 ± 0.09	stoichiometry	Wegener et al. ²⁸
	0.40 ± 0.05 (RH ≈ 32%)		Wegener et al. ²⁸
trans-2-butene	0.63 ± 0.17	LIF	this study
	0.64		IUPAC ⁵⁰
CH ₃ CHOO	0.57		MCM ³⁹
	0.64 (+0.32/−0.21)	cyclohexane	Atkinson & Aschmann ⁶⁸
	0.24 ± 0.05	stoichiometry	Horie et al. ⁷¹
	0.24 ± 0.02	CO	Gutbrod et al. ³¹
	0.68 ± 0.09	LIF (5 Torr)	Donahue et al. ²⁵
	0.54 ± 0.11	tracer	McGill et al. ⁷²
	(ca. 0.60)	LIF (low P)	Kroll et al. ³²
	0.75 ± 0.19	LIF	Siese et al. ³⁶
	0.64 ± 0.12	tracer	Orzechowski & Paulson ⁷³
	0.54 ± 0.05	tracer	Hasson et al. ⁷⁴
	0.52 ± 0.04 (RH ≈ 32%)	stoichiometry	Wegener et al. ²⁸
	0.70 ± 0.12 (RH ≈ 32%)	stoichiometry	Wegener et al. ²⁸
	0.60 ± 0.12 (RH ≈ 32%)	stoichiometry	Wegener et al. ²⁸
2,3-dimethyl-2-butene	0.83 ± 0.22	LIF	this study
	0.90		IUPAC ⁵⁰
(CH ₃) ₂ COO	1.00		MCM ³⁹
	1.00 (+0.5/−0.33)	cyclohexane	Atkinson & Aschmann ⁶⁸
	0.80 ± 0.12	2-butanol	Chew & Atkinson ³⁰

Table 2. continued

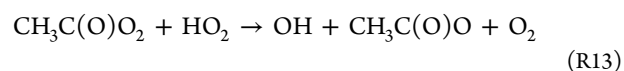
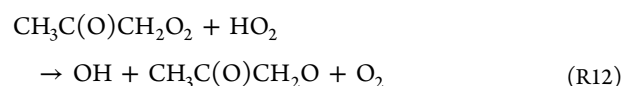
parent alkene; CIs formed	OH yield	method	ref
	0.36 ± 0.02	CO	Gutbrod et al. ³¹
	0.70 ± 0.03	LIF (5 Torr)	Donahue et al. ²⁵
	0.89 ± 0.22	tracer	Rickard et al. ²²
	0.99 ± 0.18	tracer	Fenske et al. ¹⁰
	(ca. 1.00)	LIF (low P)	Kroll et al. ³²
	1.00 ± 0.25	LIF	Siese et al. ³⁶
	0.91 ± 0.14	tracer	Orzechowski & Paulson ⁷³
	1.07 ± 0.16	2,3-butandiol	Aschmann et al. ⁷⁰

CH₂OO* CI were fixed at the values determined for ethene²⁹ for all systems, and OH yields derived as described above were used for all systems. The modeled HO₂ treatment necessarily varied between alkenes: For propene ozonolysis (see example below), any additional HO₂ formation (over and above that from CH₂OO) was assumed to result from the decomposition of CH₃CHOO*; accordingly, the branching ratio between decomposition (via the hot acid channel, producing HCHO + HO₂ + HO₂ + CO) and stabilization was optimized. The overall HO₂ yields reported here are then the sum of contributions from both CI channels. The data for 1-butene were analyzed in an equivalent manner. For *cis*-2-butene and *trans*-2-butene, CH₂OO* is not formed, and HO₂ formation within the model was constrained via the competition between decomposition through the hot acid route and CI stabilization. For 2-methylpropene, our basic understanding of the ozonolysis mechanism indicates that HO₂ formation is restricted to [CH₂OO]*. Thus, the CH₂OO decomposition products were optimized to derive an HO₂ yield for 2-methylpropene following the approach adopted previously for ethene ozonolysis.²⁹ While the hydroperoxide mechanism suggests little direct HO₂ production would be expected for 2,3-dimethyl-2-butene (all CIs are formed with a *syn*-hydrogen atom), this assumption was tested by inclusion of an HO₂-producing CI decomposition channel and optimizing the competition between this and the alternative (OH production) route.

For example, in the case of propene ozonolysis, this approach corresponds to



Interpretation of Yields Obtained. The OH and HO₂ yields obtained represent the overall yields from the fast CI decomposition chemistry (sum of both channels), relative to the flux through the initial alkene–ozone reaction, as highlighted in the reaction scheme above. It is important to note that interpretation of these yield values does not necessarily imply the production mechanism above; the data from this study do not determine the mechanistic origin of the observed HO_x radicals. The model approach in principle incorporates allowance for secondary chemical processes (thermalized bimolecular reactions), which affect HO_x abundance but does not account for potential rapid HO_x formation following the ozonolysis processes; for example, some of the detected OH production could originate from decomposition of the excited β -oxo peroxy radical.⁹ Secondary processes that were explicitly included within the model include OH formation via HO₂ + O₃ (reaction R11) and from the reactions of acyl peroxy radicals + HO₂ (reactions R12, R13)^{52–54} plus further chemistry as included within the MCM v3.2 degradation mechanisms for the parent alkenes.



4. RESULTS

Figure 3a shows a typical temporal profile of the OH steady-state concentration as measured by the LIF system and OH model simulation comparisons for *cis*-2-butene ozonolysis. These data illustrate that the MCM v3.2 overestimates (in the case of *cis*-2-butene) the OH yield, compared to the measurements obtained here; the MCM OH yield is 57%, while the yield obtained here is 27 ± 7%. [In this instance, it is likely that this arises as a 50:50 split of the two CIs assumed in the MCM 3.2 mechanism, while the lower yield obtained here (and in other studies⁵⁵) suggests that the *anti*-conformer of the CI is preferentially formed (alongside acetaldehyde) from the primary ozonide decomposition in this system.⁶ A further contribution may in principle arise from differing reactivity of the *syn*- and *anti*-CIs with H₂O at the low (but not zero) RH level of the dry experiments reported here (e.g., with H₂O)⁵⁶.] The OH yields obtained from direct observation (LIF detection

of OH) are listed in Table 2, where the reported uncertainty for the LIF data is 27%, representing combined systematic calibration uncertainty and measurement precision (2 SD). These values correspond to the overall formation of OH via the (fast) direct decomposition/isomerization of the CI, through the optimization approach described above, which takes into account secondary sources as noted above.

Figure 3b shows a typical temporal profile of the HO₂ steady-state concentration as measured by the LIF system, and HO₂ model simulation comparisons for 1-butene ozonolysis, obtained in the presence of excess CO (OH scavenger). The yields of HO₂ (Y_{HO_2}) obtained are listed in Table 3, together with equivalent values from the recent literature. The inferred Y_{HO_2} obtained in this work were found to be substantially larger, for the same chemical systems, in the absence of an OH radical scavenger (i.e., in alkene/ozone only experiments), compared

Table 3. HO₂ Yields, All under Dry Conditions (RH < 0.4%) unless Noted

parent alkene; CIs formed	HO ₂ yield	method	refe
ethene	0.10 ± 0.03	LIF	Alam et al. ²⁹ [CO system]
	0.05 ± 0.01 (RH ≈ 30%)	LIF	Alam et al. ²⁹ [CO system]
CH ₂ OO	0.13		MCM ³⁹
	0.39 ± 0.03	MIESR	Mihelcic et al. ²⁷
	0.38 ± 0.02	PERCA	Qi et al. ²⁶
	0.50 ± 0.25	stoichiometry	Wegener et al. ²⁸
propene	0.40 ± 0.20 (RH ≈ 32%)	stoichiometry	Wegener et al. ²⁸
	0.09 ± 0.02	LIF	this study
	0.02 ± 0.00 (RH ≈ 30%)	LIF	this study
CH ₂ OO	0.28		MCM ³⁹
CH ₃ CHOO	1.50 ± 0.75	stoichiometry	Wegener et al. ²⁸
	1.15 ± 0.60 (RH ≈ 32%)	stoichiometry	Wegener et al. ²⁸
	0.19 ± 0.04	PERCA	Qi et al. ³⁸
1-butene	0.18 ± 0.05	LIF	this study
	0.28		MCM ³⁹
CH ₂ OO	1.60 ± 0.80	stoichiometry	Wegener et al. ²⁸
CH ₃ CH ₂ CHOO	1.60 ± 0.80 (RH ≈ 32%)	stoichiometry	Wegener et al. ²⁸
2-methylpropene	0.34 ± 0.09	LIF	this study
	0.38 ± 0.10 (RH ≈ 30%)	LIF	this study
CH ₂ OO	0.41	MCM	MCM ³⁹
(CH ₃) ₂ COO	2.00 ± 1.00	stoichiometry	Wegener et al. ²⁸
	1.60 ± 0.80 (RH ≈ 32%)	stoichiometry	Wegener et al. ²⁸
<i>cis</i> -2-butene	0.12 ± 0.03	LIF	this study
CH ₃ CHOO	0.125	MCM	MCM ³⁹
<i>trans</i> -2-butene	0.04 ± 0.01	LIF	this study
CH ₃ CHOO	0.00 ± 0.01 (RH ≈ 30%)	LIF	this study
	0.125	MCM	MCM ³⁹
2,3-dimethyl-2-butene	0.18 ± 0.05	LIF	this study
(CH ₃) ₂ COO	0.00	MCM	MCM ³⁹
isoprene	0.16 ± 0.04	LIF	this study
CH ₂ OO, MACROOA, MVKOOA	0.26 ± 0.03	LIF	Malkin et al. ²⁴
	0.26	MCM	MCM ³⁹

with the values measured in the presence of excess CO (which effectively suppressed the OH + alkene reaction). It is likely that this reflects an interference in the LIF HO₂ radical measurements, arising from the presence of β -hydroxyalkyl peroxy radicals, formed from the reaction of OH with the parent alkene: Within the LIF sampling system, addition of NO leads to the conversion of peroxy radicals to the corresponding alkoxy species, which may then undergo further reaction (primarily with O₂ or NO as the dominant reagents present), decompose or isomerize; if these reactions lead to significant production of HO₂, on the time scale (ms) and under the conditions (<1 Torr, reduced temperature arising from the supersonic gas expansion) of the LIF system sampling chamber, a positive interference in the HO₂ measurement will result. While this conversion (e.g., via RO + O₂) has been shown⁵⁷ to be too slow to have a significant effect for small (<C₄) RO₂, recent studies⁵⁸ have shown that the interference can be significant for larger peroxy radicals (for which the reactions of the derived alkoxy radical with O₂ are faster), and in particular for the β -hydroxyalkyl peroxy radicals, such as those formed from addition of OH to alkenes; for these species, the corresponding β -hydroxyalkoxy radical reacts rapidly with O₂, forming HO₂, on the time scale of the LIF system. HO₂ interferences from peroxy radicals ranging from 0.04 (for methyl peroxy radicals, CH₃O₂) to 0.95 for β -hydroxy-propyl-peroxy radicals (CH₃CH(OH)CHO₂, formed from OH + propene) have been reported.⁵⁸ While the magnitude of the interference has been shown to vary with the specific instrument design and operational parameters (pressures, NO concentration, inlet nozzle design, and hence, gas expansion properties), the characteristics of the EUPHORE LIF system are similar to those of (one of) the systems tested⁵⁸ (0.4 mm nozzle configuration), so similar interference behavior is expected. The implication for this work is that LIF HO₂ observations performed in the absence of a radical scavenger are likely to significantly overestimate the true HO₂ concentration present; we therefore disregard these HO₂* observations from the subsequent analysis and discussion (the values obtained are included in Figure 7 for information only). Where a scavenger such as CO was used in excess (in all cases here, such that ≥97% of the OH formed reacted with the scavenger), formation of β -hydroxyalkyl peroxy radicals was essentially suppressed.

The RO₂ interference effect is clearly illustrated in Figure 4, which shows the temporal profile of HO₂ retrieved using the LIF system during the ozonolysis of propene, and the response of the measured levels to the sequential addition of CO and H₂O. Sections 1–3 of Figure 4 indicate those stages of the experiment for which only propene and ozone, and then excess CO, and then additionally H₂O (RH 30%) were present, respectively. The dashed line in Figure 4 represents the modeled HO₂ using a constant overall HO₂ yield of 0.09 (obtained using section 2 of the experiment). In all cases, the modeled OH yield was fixed at 0.36. The first stage of the experiment illustrates the β -hydroxyalkyl peroxy radical HO₂ interference effect noted above; the HO₂ levels are overestimated. Following the addition of CO, the retrieved HO₂ increases slightly (increased through the conversion of OH to HO₂, offset by removal of the interferant RO₂ species); this part of the experiment represents the base case conditions for retrieval of the actual HO₂ yield. In the third part of the experiment, water is added to increase the relative humidity to ca. 30%, and the observed HO₂ levels (shown corrected for the

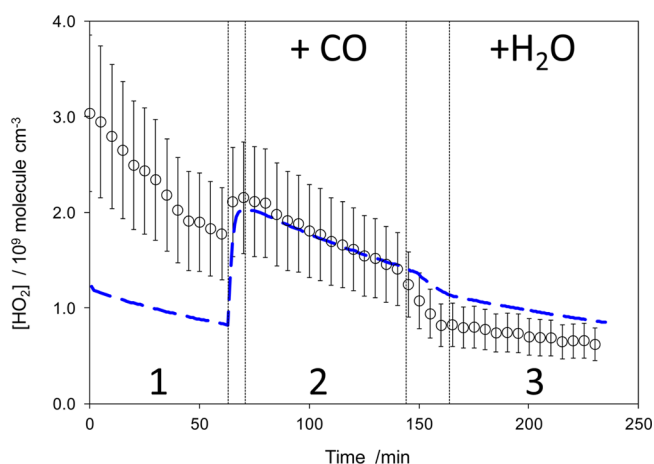


Figure 4. Observed temporal profile of HO_2 (open circles) plus model simulation during a propene ozonolysis experiment. Vertical dotted lines indicate periods during which CO and H_2O were added. During period 1, the RO_2 interference elevates the observed HO_2 (HO_2^*) above that modeled. During period 2, production of the interferant peroxy radicals is suppressed, and the measured data is used to obtain the HO_2 yield. This yield is used throughout the simulation to generate the blue dashed model line. During period 3, after the addition of H_2O , the observed HO_2 falls to a greater extent than the simulation predicts.

LIF system calibration humidity dependence) decrease. The inference from Figure 4 then is that interference effects increase the retrieved HO_2 in the absence of CO (section 1); the HO_2 yield in the absence of H_2O is 9% (section 2), and upon the addition of H_2O , the HO_2 levels decrease, potentially to a greater extent than can be accounted for by the humidity dependence of the HO_2 recombination reaction (which is included in the model), corresponding to a reduction in the HO_2 yield from propene ozonolysis with increasing humidity (section 3).

Experimental difficulties limited the PERCA observations to two chemical systems, ethene²⁹ and propene. Figure 5 shows

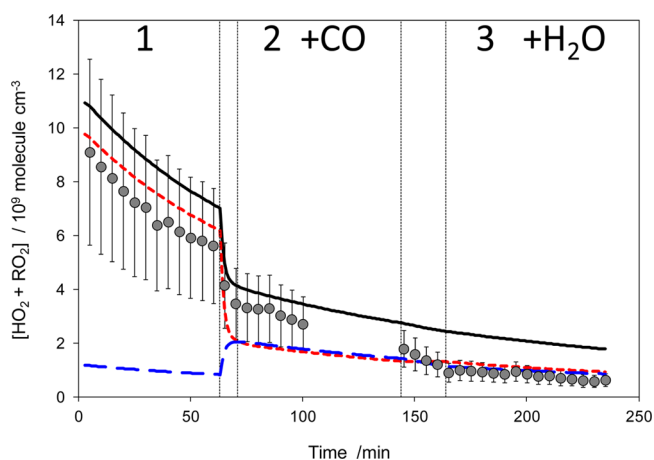


Figure 5. Measured temporal profile of $\text{HO}_2 + \Sigma\text{RO}_2$ (PERCA data, filled circles) during propene ozonolysis, plus model simulations after optimizing HO_x yields using the LIF data (PERCA data not used in optimization): blue long-dashed line, modeled HO_2 ; red short-dashed line, modeled RO_2 ; solid black line, modeled $\text{HO}_2 + \text{RO}_2$. Dotted vertical lines indicate periods during which CO and H_2O were introduced to the chamber, as in Figure 4

the observed concentrations of $\text{HO}_2 + \Sigma\text{RO}_2$ as a function of time, together with a model simulation (with OH and HO_2 yields optimized corresponding to the values given in Tables 2 and 3, respectively). As the PERCA observations were limited, we have not included these data in the yield derivation process. The modeled and observed total peroxy radical levels are in agreement, within uncertainty, during the first and second stages of the experiment. Following the increase in relative humidity from 1.3 to 20.4% (stage 3), the observed radical concentrations decrease notably, while the modeled levels are almost unaffected (the very slight change in gradient for the model trace reflecting the variation in HO_2 self-reaction rate constant with humidity, which is included in the model and indirectly affects RO_2 levels (through the $\text{RO}_2 + \text{HO}_2$ sink) in addition to HO_2 directly); the modeled HO_2/RO_2 ratio is approximately equal (to within 4%) in stages two and three. The change is consistent with the reduction in observed HO_2 levels (Figure 4) with increasing humidity, to a greater extent than can be explained by the modeled secondary chemical processes.

5. DISCUSSION

Figure 6 shows the direct OH yields obtained for ethene, propene, 1-butene, 2-methylpropene, *cis*-2-butene, *trans*-2-butene, and 2,3-dimethyl-2-butene obtained from this work, in comparison with those from other previous indirect studies plotted as a function of the equivalent IUPAC recommendations.⁵⁰ The uncertainties in the results from this work represent the combined (2σ) statistical uncertainty from repeated determinations propagated with the corresponding OH measurement calibration uncertainty. The results are well correlated with the IUPAC values; as the literature studies mainly exploit indirect methods to detect OH , by the use of OH scavenger⁵⁹ and tracer²² techniques, or indirect observation by matrix-isolation electron spin resonance²⁷ and PERCA,³⁸ the agreement with the direct OH observations in this work indicates that the overall OH radical yields from the ozonolysis of small alkenes is well characterized and that the radical data obtained here are representative of the final, long-time scale yields following relaxation of the CI system applicable to chemical modeling of the ambient atmospheric boundary layer.

The difference between the OH yields as shown in Figure 6 and a value of 1.0 reflects (a lower limit to) the formation of other products from CI decomposition and/or stabilization. In the case of 2,3-dimethyl-2-butene, all CIs formed will have the *syn* configuration and might therefore be expected to undergo the hydroperoxide mechanism rearrangement, corresponding to an OH yield of unity (the basis of the OH yield structure–activity relationship²²); however, a yield of 0.83 ± 0.22 is obtained here, in common with a number of other long time scale studies (Table 2), and non-negligible HO_2 formation is also observed (0.18 ± 0.05 ; Table 3). As OH may also be produced through other routes (e.g., by decomposition of the excited β -oxo-peroxy radical), the proportion of the CIs that do not directly yield OH may actually be somewhat larger than 17% (inferred from the corresponding OH yield of 0.83). The experimental conditions (pressure, time scale) are critical to such interpretations: Drozd et al.⁸ have illustrated the complex variation in OH and SCI production from 2,3-dimethyl-2-butene ozonolysis, showing that time- and pressure-dependent OH yields arise from at least two decomposition vs. stabilization routes, from the initial SCI and the vinyl-

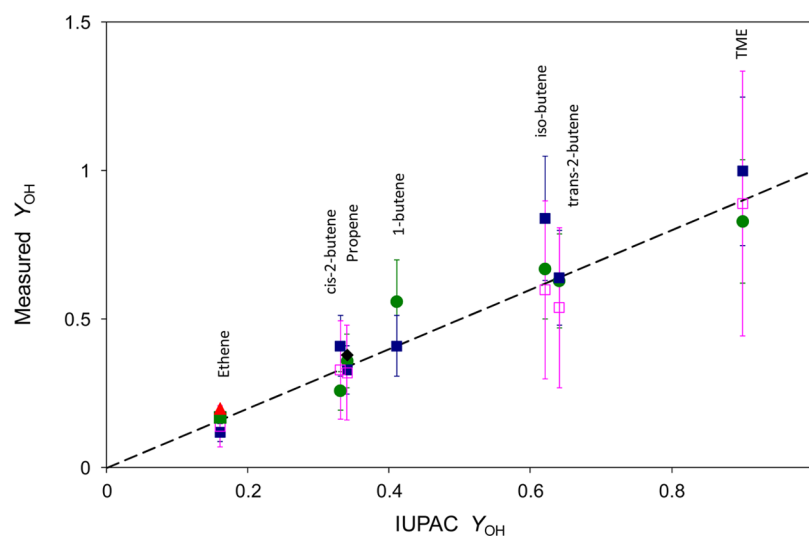


Figure 6. Comparison of measured OH yields from this work and selected literature studies vs. IUPAC OH yield recommendations. Filled green circles, this work; filled blue squares, Atkinson et al.,⁵⁹ cyclohexane scavenger; open magenta circles, Marston and co-workers,^{22,72} TMB scavenger; filled black diamond, Qi et al.,³⁸ PERCA; filled red triangle, Mihelcic et al.,²⁷ MIESR. The dashed line shows the 1:1 correlation.

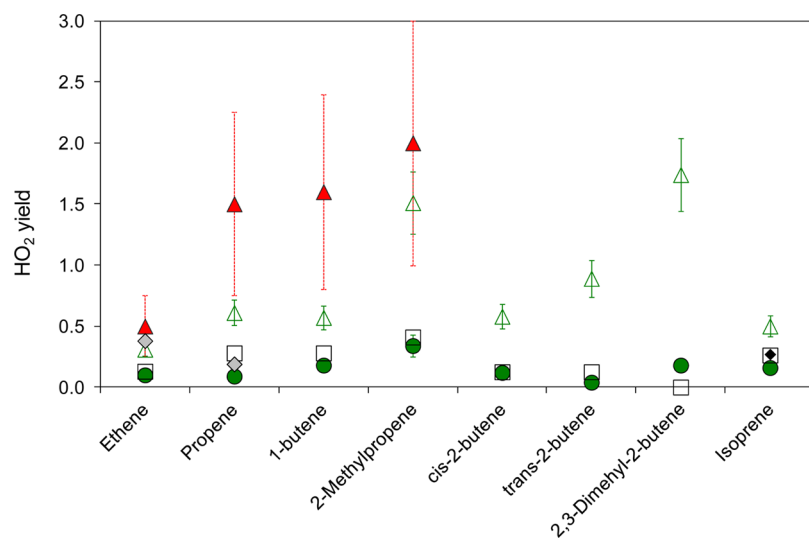


Figure 7. Comparison of HO₂ yields for small chain alkenes investigated during this study with literature. Filled green circles and open green triangles are HO₂ yields calculated from this study (by LIF) for excess CO and non-scavenged (i.e., with RO₂ interference) experiments, respectively. Filled red triangles, Wegener et al.;²⁸ open black squares, MCM v3.2; gray diamonds, Qi et al.;^{26,38} black diamond, Malkin et al.;²⁴ black star, Mihelcic et al.²⁷

hydroperoxide intermediate. Berndt et al.⁶⁰ have recently reported an SCI yield of 0.62 ± 0.28 for 2,3-dimethyl-2-butene, obtained from measurement of the H₂SO₄ formed from SCI + SO₂ reactions at atmospheric pressure and on a time scale of 0.5–1.5 s. The difference between this value and $(1 - Y_{\text{OH}})$ values obtained from this work and other studies (Table 2) may therefore reflect the different time scales probed, with further OH production occurring from thermalized SCI decomposition occurring at longer time scales³ (although a humidity dependence to the OH yield might then be expected, from competition between SCI decomposition and reaction with H₂O, in contrast to the majority of literature studies, see discussion below). This in turn would indicate that the yield of SCIs formed in the atmospheric boundary layer from alkene ozonolysis (and available to undergo bimolecular reactions with other species) may be somewhat lower than measurements performed in short-time scale laboratory studies indicate.

The HO₂ yields obtained here (Table 3) range from 0.01 for *trans*-2-butene to 0.34 for 2-methylpropene (in experiments where excess CO was present, and hence, LIF HO₂ interference effects did not occur), suggesting that HO₂ production can be a significant proportion of the total ozonolysis radical yield for some systems but that it is not formed at yields approaching unity or above, consistent with HO₂ production from the *anti*-CI, and in effective competition with other fates such as stabilization, other decomposition pathways and bimolecular reaction. Nonzero HO₂ production was observed for the 2,3-dimethyl-2-butene system, where all CIs will form in a *syn* configuration amenable to the hydroperoxide rearrangement, pointing to some scope for HO₂ formation from *syn*-CIs, in competition with OH, potentially via the hot acid intermediate (Figure 2).

The literature database of experimental measurements of production of HO₂ from alkene ozonolysis is sparse in

comparison with that for OH. The HO₂ yield for propene ozonolysis obtained here (0.09 ± 0.02) is lower than the value obtained by Qi et al.³⁸ of 0.19 ± 0.04 , and substantially below the values obtained by Wegener et al.²⁸ of 1.50 ± 0.75 and 1.15 ± 0.60 (dry and humid, respectively). The HO₂ yields for 1-butene and 2-methylpropene obtained here are also substantially lower than the corresponding values reported by Wegener et al. (Table 3). Qi et al. comment that their results were sensitive to the assumed distribution of radical products (OH/HO₂/CH₃O₂) within the model used to interpret the PERCA data, and analyzed their data assuming an SCI yield from CH₂OO of 0.37, substantially lower than the 0.54 found elsewhere.²⁹ While full details of the 58-reaction chemical scheme used to interpret the experimental data and the sensitivity of the inferred yields to the mechanistic assumptions are not given, it is possible that a corresponding increase in the stabilization yield for CH₂OO would result in lower inferred radical production in their study. For isoprene, the result obtained here (0.16 ± 0.04) is somewhat lower than the only other value directly measured, 0.26 ± 0.03 ,²⁴ obtained using a comparable chamber ozonolysis–LIF observation approach, but in the absence of a scavenger, which may have led to an interference contribution to the measured HO₂ from hydroxyl-substituted peroxy radicals.

It is difficult to reconcile some very high HO₂ yields from the literature with the other product yields measured in this and other studies; for example, in the case of 2-methylpropene, the inferred yield²⁹ of the two CI species is 34:66 for (CH₃)₂COO*/CH₂OO*, while the measured HO₂ yield from ethene (i.e., from the CH₂OO* CI) ranges from 0.10 to 0.40.^{27,29} As the (CH₃)₂COO* CI would be expected to always undergo a hydroperoxide rearrangement to produce predominantly OH (and indeed OH yields in the range 0.6–0.8 are observed, see Figure 6), with limited HO₂ coproduction (as noted above), HO₂ yields from 2-methylpropene (from CH₂OO*, or from (CH₃)₂COO* undergoing alternative minor decomposition pathways) would be expected to be of the order of 0.3–0.5, rather than the (2.00 ± 1.00) measured by Wegener et al.²⁸ Although the measurements made using the additional turnover approach suffer from relatively low precision in comparison with the LIF observations, the discrepancy is greater than the (combined) uncertainties of both studies.

The variation in HO_x yields with humidity was studied for a subset of systems (Tables 2 and 3). Experimental difficulties (partial failure of the LIF system pump laser) limited the data obtained for OH; however, for HO₂, reduced production with increasing humidity was observed for propene and *trans*-2-butene (albeit from a very low level in the latter case), while no change (within uncertainty) was observed for 2-methylpropene. The reduction in yield for propene was replicated in the (independent) LIF and PERCA measurements (Figures 4 and 5), consistent with the behavior observed previously for the ethene system²⁹ producing the CH₂OO CI in common with other terminal alkenes. Both the LIF and PERCA instruments used in this work exhibit known humidity-dependent sensitivities/calibrations, which were taken into account in the data analysis; an error in this factor is considered unlikely for the LIF HO₂ data, which would otherwise be expected to show a systematic humidity bias across all the chemical/alkene systems considered, but cannot be precluded on the same basis for the PERCA instrument, for which only very limited observations (on a single system) were possible. One further

caveat is that the interpretation presented here is that the humidity dependence lies in the HO₂ yields. Equivalent measurements of the OH yields with humidity were not available from this study, consequently, this mechanistic interpretation is based upon the balance of the literature regarding OH production (discussed below); in principle a change in the OH yields with humidity could also contribute to the observed trend.

The majority of published indirect experimental tracer/scavenger studies find OH yields from alkene ozonolysis to remain unaffected under enhanced humidity,^{14,23} indicating that either the water reaction is not competitive with decomposition or forms products that also decompose to yield OH, e.g., an unstable hydroperoxide.⁶¹ Kuwata et al.⁶² predict that the hydroperoxide mechanism (thought to be the principal source of OH) proceeds 3–8 orders of magnitude faster than the thermalized CI reaction with water for stabilized *syn*-CIs, under typical tropospheric conditions (*T*, *P*, and humidity), but that unimolecular rearrangement to dioxirane occurs at a comparable rate to the bimolecular reaction with water for the *anti*-CI conformer of methyl carbonyl oxide (CH₃CHOO), raising the possibility for water to affect radical production from this conformer. Kroll et al.⁶³ investigated the possibility of OH formation from the *anti*-CI by measuring yields of OD and OH radicals from deuterated (and undeuterated) *cis*- and *trans*-3-hexene, concluding that OH formation from *anti*-CIs may also play a significant role in the total OH yield, as approximately one-third of the total OH yield comes from the *anti*-CI in the ozonolysis of *cis*-3-hexene. Drozd et al.⁸ have shown that increasing alkene/CI size/carbon number substantially increases SCI stabilization for internal alkenes, indicating that competition between stabilization and OH production is likely to be strongly species/conformer dependent; indeed, an increase in OH yield with humidity (0.02% to 45% RH) for α -pinene using the cyclohexane scavenger approach has been reported,⁶⁴ attributed to decomposition of the SCI + H₂O formed hydroxyl-hydroperoxide, but subject also to assumptions regarding the contribution of HO₂ (potentially also changing with humidity) and variations in the cyclohexanone/cyclohexanol yields in the presence of varying HO₂/RO₂ populations.²⁹ Wegener et al.²⁸ reported positive humidity dependence for OH formation (increasing production with increasing H₂O) for a number of small alkenes, where yields were obtained through assessment of the additional turnover of the parent alkene. It is hard to reconcile these results with the tracer/scavenger studies for small alkenes reported above; Wegener et al. speculate that the humidity dependence observed in their study, which corresponds to better agreement between their humid OH yields and those observed in (literature) dry experiments, may reflect ambient water vapor entering the experimental systems used in other literature studies, which are effectively therefore somewhat wet; an effect minimized in the double-walled SAPHIR chamber (in the present study, where the single-walled EUPHORE chamber was used, but maintained at above-ambient pressure, leaks led to a reduction in RH (for elevated H₂O experiments) as the chamber air was replaced by dry scrubbed air). Future studies of ozonolysis product yields should directly measure the humidity within the experimental chamber in question to address this possibility.

The observed variation in HO₂ yields with humidity from this work is consistent with a humidity-dependent radical production from the CH₂OO CI formed from all terminal

alkenes but suggest that H₂O exerts little influence in HO₂ production from the C₂ CH₃CHOO CIs formed in the *cis*- and *trans*-2-butene systems. In the case of 2-methylpropene, the relative yields of the (CH₃)₂CHOO and CH₂OO CIs are 66/34%,⁵¹ such that the variation in the small contribution to HO₂ from the CH₂OO moiety would lie within the uncertainty of the measurements for this parent alkene overall (Table 3). This interpretation is consistent with theoretical predictions,⁶⁵ which found that reaction of the *anti*-CI CH₃CHOO (the postulated predominant precursor to the HO₂ observed) with water occurs several orders of magnitude faster than the equivalent reaction for the *syn*-CH₃CHOO, or (CH₃)₂CHOO and is supported by recent direct measurement of SCI + H₂O rate constants for the *syn*- and *anti*-conformers of CH₃CHOO of $<4 \times 10^{-15}$ and 1×10^{-14} molec⁻¹ cm³ s⁻¹, respectively.⁵⁶ The only other reported measurement of the humidity dependence of HO₂ production, from Wegener et al., found no change in HO₂ production for ethene, propene, 1-butene, and isobutene between 100 and ca. 10000 ppm H₂O (RH levels of approximately 0.3 and 32%, respectively) but with substantial uncertainty (50%), which would encompass the variation reported here (Table 3).

The results of this work indicate a generally consistent understanding of OH yields from the ozonolysis of small alkenes, consistent with the predominance of the hydroperoxide mechanism, but with some indications (e.g., subunity yield for 2,3-dimethyl-2-butene) that other fates are possible for *syn*-CIs and (from the observation of OH production from ethene) that other primary OH formation routes occur. It seems unlikely that there is a substantial humidity dependence to ozonolysis OH yields, at least for the small ($\leq C_5$) alkenes considered here, but the contradictory results of recent studies require further definitive confirmation of this aspect. The HO₂ yields obtained here (in experiments where excess CO was present and hence LIF HO₂ interference effects eliminated) range from 0.01 (*trans*-2-butene) to 0.34 (2-methylpropene), suggesting that HO₂ production can be a significant proportion of the total ozonolysis radical yield for some systems but that it is not formed at yields approaching unity or above, consistent with HO₂ production from the *anti*-CI, through the hot acid intermediate, in competition with stabilization and other degradation products. The reduction in HO₂ formation with increasing humidity observed for the ethene, propene, and *trans*-2-butene systems are consistent with theoretical studies indicating that reaction with H₂O can be competitive with dissociation for the CH₃CHOO *anti*-CI. Following the argument of Wegener et al. regarding the water level present in the chamber under nominally dry conditions, considering the humidity range probed here (where dry conditions correspond to [H₂O] = 2.7×10^{15} molecules cm⁻³; RH = 0.35%; and wet to [H₂O] = 2.4×10^{17} molecules cm⁻³; RH = 30%), it may be that higher HO₂ yields would be observed under totally dry conditions and that the yields applicable to the ambient atmospheric boundary layer (where higher RH is frequently encountered) will be lower than those reported here, which could then be regarded as upper limits.

The impact of the measured yields for atmospheric OH and HO₂ production was evaluated using a photochemical box model simulation of boundary layer composition under polluted suburban conditions. A zero-dimensional box model simulation was performed using the MCM (v3.2) mechanism, with radical yields updated following Tables 2 and 3, for five C₂–C₅ alkanes, seven C₂–C₆ alkenes, isoprene, methanol,

ethanol, formaldehyde, and acetaldehyde. Initial concentrations of these parent volatile organic compounds (VOCs) were set to the mean values observed during the TORCH field campaign in Chelmsford, a suburban location downwind of London, during summer 2003;⁶⁶ the parent VOC species used accounted for 92% of the total calculated OH reactivity from all measured species. NO_x, O₃, CO, CH₄, temperature, and RH conditions were set to median values of those observed, while photolysis rates were calculated for clear sky conditions. Following spin-up, the model was used to quantify mean radical production rates over two three-hour periods, from 12.00 to 15.00 and 24.00–03.00 h local time. During daytime, 71% of OH primary production arose from O₃ photolysis/O(¹D) + H₂O reaction, while 29% arose from alkene ozonolysis, consistent with previous results,⁴ as might be expected considering the similarity in measured OH yields to those implemented within the MCM. Daytime primary HO₂ production was dominated by photolysis of HCHO (84%) with photolysis of other carbonyl species accounting for 12% and alkene ozonolysis contributing 4% of the total. At night, ozonolysis dominated OH and HO₂ production. Under both conditions, reaction of 2,3-dimethyl-2-butene was the single most significant ozonolysis contribution, accounting for ca. 45% of the total ozonolysis contribution, at least under the conditions of the TORCH measurements. These calculations do not include a contribution from HONO photolysis, which was not measured during TORCH but has been shown to make a very important contribution to photolytic OH production in the boundary layer.⁶⁷

6. CONCLUSIONS

The OH and HO₂ yields from the ozonolysis of a range of small C₂–C₅ alkenes have been measured using large simulation chamber experiments incorporating direct measurement of OH and HO₂ by laser-induced fluorescence (LIF) and HO₂ + RO₂ by peroxy radical chemical amplification (PERCA). The direct yields of OH obtained here are consistent with those reported in the literature as obtained indirectly by tracer/scavenger studies on long time scales relevant to the atmospheric boundary layer and are similar to those currently used in atmospheric models. The LIF HO₂ measurements were found to be substantially influenced by an interference from hydroxyl-peroxy radicals, formed from OH addition to the parent alkene, other than in experiments where an OH scavenger (CO) was employed. The yields of HO₂ obtained in such experiments are lower than the limited number of previous studies suggest and are somewhat lower than those used in the Master Chemical Mechanism (MCM v3.2), indicating that total radical production from alkene ozonolysis may be somewhat less than currently calculated using this and other comparable mechanisms. A reduction in HO₂ formation with increasing humidity was observed, indicating that the values obtained might be regarded as upper limits under ambient atmospheric boundary layer conditions, with the caveat that this conclusion depends in part upon applying humidity-independent OH yields to the data, based upon past literature results. The observed OH and HO₂ formation is consistent with the hydroperoxide mechanism dominating (but not exclusively) the evolution of *syn*-CIs, and with HO₂ formation occurring primarily through decomposition of *anti*-CIs and the CH₂OO CI formed from terminal alkenes, in a competition with reaction with water vapor, and potentially other atmospheric trace gases.

■ AUTHOR INFORMATION

Present Addresses

^{||}(A.R.R.) National Centre for Atmospheric Science, Wolfson Atmospheric Chemistry Laboratory, Department of Chemistry, University of York, York YO10 5DD, U.K.

[⊥](M.C.) LISA, UMR CNRS/INSU 7583, Université Paris Est Créteil et Université Paris Diderot, Institut Pierre Simon Laplace, 94010 Créteil Cedex, France.

[#](K.P.W.) School of Environment and Technology, University of Brighton, Brighton BN2 4GJ, U.K.

[○](K.E.H.) Department of Geological Sciences, Indiana University, Bloomington, Indiana 47405, United States.

Notes

The authors declare no competing financial interest.

■ ACKNOWLEDGMENTS

We would like to thank co-workers from Fundação CEAM, Valencia and Dr. Roland Leigh, Dr. Zoë Fleming, and Dr. Iain White from the University of Leicester for technical support during the TRAPOZ experiments performed at EUPHORE and subsequent data analysis. The TRAPOZ project was funded by the U.K. Natural Environment Research Council (Grant ref NE/E016081/1).

■ REFERENCES

- (1) Calvert, J. G.; Atkinson, R.; Kerr, J. A.; Madronich, S.; Moortgat, G. K.; Wallington, T. J.; Yarwood, G. *The Mechanism of Atmospheric Oxidation of the Alkenes*; Oxford University Press: New York, 2000.
- (2) Di Carlo, P.; Brune, W. H.; Martinez, M.; Harder, H.; Leshner, R.; Ren, X.; Thornberry, T.; Carroll, M. A.; Young, V.; Shepson, P. B.; et al. Missing OH Reactivity in a Forest: Evidence for Unknown Reactive Biogenic VOCs. *Science* **2004**, *302*, 722–725.
- (3) Johnson, D.; Marston, G. The Gas-Phase Ozonolysis of Unsaturated Volatile Organic Compounds in the Troposphere. *Chem. Soc. Rev.* **2008**, *37*, 699–716.
- (4) Emmerson, K. M.; Carslaw, N.; Carslaw, D. C.; Lee, J. D.; McFiggans, G.; Bloss, W. J.; Gravesstock, T.; Heard, D. E.; Hopkins, J.; Ingham, T.; et al. Free Radical Modelling Studies during the UK TORCH Campaign in Summer 2003. *Atmos. Chem. Phys.* **2007**, *7*, 167–181.
- (5) Criegee, R. Mechanism of Ozonolysis. *Angew. Chem., Int. Ed.* **1975**, *14*, 745–752.
- (6) Rathman, W. C. D.; Claxton, T. A.; Rickard, A. R.; Marston, G. A Theoretical Investigation of OH Formation in the Gas-Phase Ozonolysis of *E*-but-2-ene and *Z*-but-2-ene. *Phys. Chem. Chem. Phys.* **1999**, *1*, 3981–3985.
- (7) Niki, H.; Maker, P. D.; Savage, C. M.; Breitenbach, L. P.; Hurley, M. FTIR Spectroscopic Study of the Mechanism for the Gas-Phase Reaction between Ozone and Tetramethylethylene. *J. Phys. Chem.* **1987**, *91*, 941–946.
- (8) Drozd, G. T.; Kroll, J.; Donahue, N. M. 2,3-Dimethyl-2-butene (TME) Ozonolysis: Pressure Dependence of Stabilized Criegee Intermediates and Evidence of Stabilized Vinyl Hydroperoxides. *J. Phys. Chem. A* **2011**, *115*, 161–166.
- (9) Kuwata, K. T.; Hasson, A. S.; Dickinson, R. V.; Petersen, E. B.; Valin, L. C. Quantum Chemical and Master Equation Simulations of the Oxidation and Isomerization of Vinyloxy Radicals. *J. Phys. Chem. A* **2005**, *109*, 2514–2524.
- (10) Fenske, D.; Hasson, A. S.; Paulson, S. E.; Kuwata, K. T.; Ho, A.; Houk, A. N. The Pressure Dependence of the OH Radical Yield from Ozone–Alkene Reactions. *J. Phys. Chem. A* **2000**, *104*, 7821–7833.
- (11) Olzmann, M.; Kraka, E.; Cremer, D.; Gutbrod, R.; Andersson, S. Energetics, Kinetics, and Product Distributions of the Reactions of Ozone with Ethene and 2,3-Dimethyl-2-butene. *J. Phys. Chem. A* **1997**, *101*, 9421–9429.

(12) Kurtén, T.; Donahue, N. M. MRCISD Studies of the Dissociation of Vinylhydroperoxide, CH₂CHOOH: There Is a Saddle Point. *J. Phys. Chem. A* **2012**, *116*, 6823–6830.

(13) Hatakeyama, S.; Akimoto, H. Reactions of Criegee Intermediates in the Gas Phase. *Res. Chem. Intermed.* **1994**, *20*, 503–524.

(14) Johnson, D.; Lewin, A. G.; Marston, G. The Effect of Criegee-Intermediate Scavengers on the OH Yield from the Reaction of Ozone with 2-Methylbut-2-ene. *J. Phys. Chem. A* **2001**, *105*, 2933–2935.

(15) Welz, O.; Savee, J. D.; Osborn, D. L.; Vasu, S. S.; Percival, C. J.; Shallcross, D. E.; Taatjes, C. A. Direct Kinetic Measurements of Criegee Intermediate (CH₂OO) Formed by Reaction of CH₂I with O₂. *Science* **2012**, *335*, 204–207.

(16) Mauldin, R. L., III; Berndt, T.; Sipilä, M.; Paasonen, P.; Petäjä, T.; Kim, S.; Kurtén, T.; Stratmann, F.; Kerminen, V.-M.; Kulmala, M. A New Atmospherically Relevant Oxidant of Sulphur Dioxide. *Nature* **2012**, *488*, 193–197.

(17) Ouyang, B.; McLeod, M. W.; Jones, R. L.; Bloss, W. J. NO₃ Radical Production from the Reaction between the Criegee Intermediate CH₂OO and NO₂. *Phys. Chem. Chem. Phys.* **2013**, *15*, 17070–17075.

(18) Finlayson, B. J.; Pitts, J. N.; Atkinson, R. Low-Pressure Gas Phase Ozone–Olefin Reactions: Chemiluminescence, Kinetics and Mechanisms. *J. Am. Chem. Soc.* **1974**, *96*, 5356–5367.

(19) Herron, J. T.; Huie, R. E. Stopped-Flow Studies of the Mechanisms of Ozone–Alkene Reactions in the Gas Phase Propene and Isobutene. *Int. J. Chem. Kinet.* **1978**, *10*, 1019–1041.

(20) Martinez, R. I.; Herron, J. T.; Huie, R. E. The Mechanism of Ozone–Alkene Reactions in the Gas Phase. A Mass Spectrometric Study of the Reactions of Eight Linear and Branched-Chain Alkenes. *J. Am. Chem. Soc.* **1981**, *103*, 3807–3820.

(21) Paulson, S. E.; Chung, M. Y.; Hasson, A. S. OH Radical Formation from the Gas-Phase Reaction of Ozone with Terminal Alkenes and the Relationship between Structure and Mechanism. *J. Phys. Chem. A* **1999**, *103*, 8125–8138.

(22) Rickard, A. R.; Johnson, D.; McGill, C. D.; Marston, G. OH Yields in the Gas-Phase Reactions of Ozone with Alkenes. *J. Phys. Chem. A* **1999**, *103*, 7656–7664.

(23) Atkinson, R.; Aschmann, S. M.; Arey, J.; Shorees, B. Formation of OH Radicals in the Gas-Phase Reactions of O₃ with a Series of Terpenes. *J. Geophys. Res.* **1992**, *97*, 6065–6073.

(24) Malkin, T. L.; Goddard, A.; Heard, D. E.; Seakins, P. W. Measurements of OH and HO₂ Yields from the Gas Phase Ozonolysis of Isoprene. *Atmos. Chem. Phys.* **2010**, *10*, 1441–1459.

(25) Donahue, N. M.; Kroll, J. H.; Anderson, J. G.; Demerjian, K. L. Direct Observation of OH Production from the Ozonolysis of Olefins. *Geophys. Res. Lett.* **1998**, *25*, 59–62.

(26) Qi, B.; Sato, K.; Imarnura, T.; Takami, A.; Hatakeyama, S.; Ma, Y. Production of the Radicals in the Ozonolysis of Ethene: A Chamber Study by FT-IR and PERCA. *Chem. Phys. Lett.* **2006**, *427*, 461–465.

(27) Mihelcic, D.; Heitlinger, M.; Kley, D.; Musgen, P.; Volz-Thomas, A. Formation of Hydroxyl and Hydroperoxy Radicals in the Gas-Phase Ozonolysis of Ethane. *Chem. Phys. Lett.* **1999**, *301*, 559–564.

(28) Wegener, R.; Brauers, T.; Koppmann, R.; Bares, S. R.; Rohrer, F.; Tillmann, R.; Wahner, A.; Hansel, A.; Wisthaler, A. Simulation Chamber Investigation of the Reactions of Ozone with Short-Chain Alkenes. *J. Geophys. Res.* **2007**, *112*, D13301.

(29) Alam, M. S.; Camredon, M.; Rickard, A. R.; Carr, T.; Wyche, K. P.; Hornsby, K. E.; Monks, P. S.; Bloss, W. J. Total Radical Yields from Tropospheric Ethene Ozonolysis. *Phys. Chem. Chem. Phys.* **2011**, *13*, 11002–11015.

(30) Chew, A. A.; Atkinson, R. OH Radical Formation Yields from the Gas Phase Reactions of O₃ with Alkenes and Monoterpenes. *J. Geophys. Res.* **1996**, *101*, 28649–28653.

(31) Gutbrod, R.; Meyer, S.; Rahman, M. M.; Schindler, R. N. On the Use of CO as Scavenger for OH Radicals in the Ozonolysis of Simple Alkenes and Isoprene. *Int. J. Chem. Kinet.* **1997**, *29*, 717–723.

(32) Kroll, J. H.; Hanisco, T. F.; Donahue, N. M.; Demerjian, K. L.; Anderson, J. G. Accurate, Direct Measurements of OH Yields from

Gas-Phase Ozone–Alkene Reactions using an in Situ LIF Instrument. *Geophys. Res. Lett.* **2001**, *28*, 3863–3866.

(33) Kroll, J. H.; Clarke, J. S.; Donahue, N. M.; Anderson, J. G.; Demerjian, K. L. Mechanism of HO_x Formation in the Gas-Phase Ozone–Alkene Reaction. 1. Direct, Pressure-Dependent Measurements of Prompt OH Yields. *J. Phys. Chem. A* **2001**, *105*, 1554–1560.

(34) Kroll, J. H.; Sahay, S. R.; Anderson, J. G.; Demerjian, K. L.; Donahue, N. M. Mechanism of HO_x Formation in the Gas-Phase Ozone–Alkene Reaction. 2. Prompt versus Thermal Dissociation of Carbonyl Oxides to form OH. *J. Phys. Chem. A* **2001**, *105*, 4446–4457.

(35) Presto, A.; Donahue, N. Ozonolysis Fragment Quenching by Nitrate Formation: The Pressure Dependence of Prompt OH Radical Formation. *J. Phys. Chem. A* **2004**, *108*, 9096–9104.

(36) Siese, M.; Becker, K. H.; Brockmann, K. J.; Geiger, H.; Hofzumahaus, A.; Holland, F.; Milhelcic, M.; Wirtz, K. Direct Measurement of OH Radicals from Ozonolysis of Selected Alkenes: A EUPHORE Simulation Chamber Study. *Environ. Sci. Technol.* **2001**, *35*, 4660–4667.

(37) Paulson, S. E.; Orlando, J. J. The Reactions of Ozone with Alkenes: An Important Source of HO_x in the Boundary Layer. *Geophys. Res. Lett.* **1996**, *23*, 3727–3730.

(38) Qi, B.; Yang, B.; Wang, Z. Q.; Yang, H. Y.; Liu, L. Production of Radicals in the Ozonolysis of Propene in Air. *Sci. China, Ser. B: Chem.* **2009**, *52*, 356–361.

(39) Jenkin, M. E.; Saunders, S. M.; Pilling, M. J. The Tropospheric Degradation of Volatile Organic Compounds: A Protocol for Mechanism Development. *Atmos. Environ.* **1997**, *31*, 81–104.

(40) Becker, K. H. In Situ Euphore Radical Measurement (EUROPHAM): Report to the European Commission, Contract ENV4-CT95-0011; Bergische Universität Wuppertal: Germany, 1999.

(41) Camredon, M.; Hamilton, J. F.; Alam, M. S.; Wyche, K. P.; Carr, T.; White, I. R.; Monks, P. S.; Rickard, A. R.; Bloss, W. J. Distribution of Gaseous and Particulate Organic Composition during Dark Alphapinene Ozonolysis. *Atmos. Chem. Phys.* **2010**, *10*, 2893–2917.

(42) Bloss, W. J.; Lee, J. D.; Bloss, C.; Heard, D. E.; Pilling, M. J.; Wirtz, K.; Martin-Reviejo, M.; Siese, M. Validation of the Calibration of a Laser-Induced Fluorescence Instrument for the Measurement of OH Radicals in the Atmosphere. *Atmos. Chem. Phys.* **2004**, *4*, 571–583.

(43) Green, T. J.; Reeves, C. E.; Fleming, Z. L.; Brough, N.; Rickard, A. R.; Bandy, B. J.; Monks, P. S.; Penkett, S. A. An Improved Dual Channel PERCA Instrument for Atmospheric Measurements of Peroxy Radicals. *J. Environ. Monit.* **2006**, *8*, 530–536.

(44) Aschmutat, U.; Hessling, M.; Holland, F.; Hofzumahaus, A. *Physico-Chemical Behaviour of Atmospheric Pollutants*; Angeletti, G.; Restelli, C.; Proc. EUR 15609; Wiley: New York, 1994; pp 811–816.

(45) Creasey, D. J.; Halford-Maw, P. A.; Heard, D. E.; Pilling, M. J.; Whitaker, B. J. Implementation and Initial Deployment of a Field Instrument for Measurement of OH and HO₂ in the Troposphere by Laser-Induced Fluorescence. *J. Chem. Soc., Faraday Trans.* **1997**, *93*, 2907–2913.

(46) Clemitshaw, K. C.; Carpenter, L. J.; Penket, S. A.; Jenkin, M. J. A Calibrated Peroxy Radical Chemical Amplifier for Ground-Based Tropospheric Measurements. *J. Geophys. Res.* **1997**, *102*, 25405–25416.

(47) Fleming, Z. L.; Monks, P. S.; Rickard, A. R.; Heard, D. E.; Bloss, W. J.; Seakins, P. W.; Still, T. J.; Sommariva, R.; Pilling, M. J.; Morgan, R.; et al. Peroxy Radical Chemistry and the Control of Ozone Photochemistry at Mace Head, Ireland during the Summer of 2002. *Atmos. Chem. Phys.* **2006**, *6*, 2193–2214.

(48) Saunders, S. M.; Jenkin, M. E.; Derwent, R. G.; Pilling, M. J. Protocol for the Development of the Master Chemical Mechanism, MCM v3 (Part A): Tropospheric Degradation of Non-Aromatic Volatile Organic Compounds. *Atmos. Chem. Phys.* **2003**, *3*, 161–180.

(49) Curtis, A. R.; Sweetenham, W. P. Facsimile/Checkmat User's Manual; Harwell Laboratory: Oxfordshire, U.K., 1987.

(50) IUPAC: Subcommittee for Gas Kinetic Data Evaluation, 1999. <http://www.iupac-kinetic.ch.cam.ac.uk>.

(51) Alam, M. S. Ph.D. Thesis, University of Birmingham, 2011.

(52) Dillon, T. J.; Crowley, J. N. Direct Detection of OH Formation in the Reactions of HO₂ with CH₃C(O)O₂ and other Substituted Peroxy Radicals. *Atmos. Chem. Phys.* **2008**, *8*, 4877–4889.

(53) Hasson, A. S.; Tyndall, G. S.; Orlando, J. J. A Product Yield Study of the Reaction of HO₂ Radicals with Ethyl Peroxy (C₂H₅SO₂), Acetyl Peroxy (CH₃C(O)O₂), and Acetonyl Peroxy (CH₃C(O)-CH₂O₂) Radicals. *J. Phys. Chem. A* **2004**, *108*, 5979–5989.

(54) Jenkin, M. E.; Hurley, M. D.; Wallington, T. J. Investigation of the Radical Product Channel of the CH₃C(O)O₂ + HO₂ Reaction in the Gas Phase. *Phys. Chem. Chem. Phys.* **2007**, *9*, 3149–3162.

(55) Atkinson, R.; Baulch, D. L.; Cox, R. A.; Crowley, J. N.; Hampson, R. F.; Hynes, R. G.; Jenkin, M. E.; Rossi, M. J.; Troe, J. Evaluated Kinetic and Photochemical Data for Atmospheric Chemistry: Volume II, Gas Phase Reactions of Organic Species. *Atmos. Chem. Phys.* **2006**, *6*, 3625–4055.

(56) Taatjes, C. A.; Welz, O.; Eskola, A. J.; Savee, J. D.; Scheer, A. M.; Shallcross, D. E.; Rotavera, B.; Lee, E. P. F.; Dyke, J. M.; Mok, D. K. W.; et al. Direct Measurements of Conformer-Dependent Reactivity of the Criegee Intermediate CH₃CHOO. *Science* **2013**, *340*, 177–180.

(57) Heard, D. E.; Pilling, M. J. Measurement of OH and HO₂ in the Troposphere. *Chem. Rev.* **2003**, *103*, 5163–5198.

(58) Fuchs, H.; Bohn, B.; Hofzumahaus, A.; Holland, F.; Lu, K. D.; Nehr, S.; Rohrer, F.; Wahner, A. Detection of HO₂ by Laser-Induced Fluorescence: Calibration and Interferences from RO₂ Radicals. *Atmos. Meas. Tech.* **2011**, *4*, 1209–1225.

(59) Atkinson, R. Gas-Phase Tropospheric Chemistry of Volatile Organic Compounds: 1. Alkanes and Alkenes. *J. Phys. Chem. Ref. Data* **1997**, *26*, 215–290.

(60) Berndt, T.; Jokinen, T.; Mauldin, R. L., III; Petäjä, T.; Herrmann, H.; Junninen, H.; Paasonen, P.; Worsnop, D.; Sipilä, M. Gas-Phase Ozonolysis of Selected Olefins: The Yield of Stabilized Criegee Intermediate and the Reactivity toward SO₂. *J. Phys. Chem. Lett.* **2012**, *3*, 2892–2896.

(61) Anglada, J. M.; Aplincourt, P.; Bofill, J. M.; Cremer, D. Atmospheric Formation of OH Radicals and H₂O₂ from Alkene Ozonolysis under Humid Conditions. *ChemPhysChem* **2002**, *3*, 215–221.

(62) Kuwata, K. T.; Hermes, M. R.; Carlson, M. J.; Zogg, C. K. Computational Studies of the Isomerization and Hydration Reactions of Acetaldehyde Oxide and Methyl Vinyl Carbonyl Oxide. *J. Phys. Chem. A* **2010**, *114*, 9192–9204.

(63) Kroll, J. H.; Donahue, N. M.; Cee, V. J.; Demerjian, K. L.; Anderson, J. G. Gas-Phase Ozonolysis of Alkenes: Formation of OH from Anti Carbonyl Oxides. *J. Am. Chem. Soc.* **2002**, *124*, 8518–8519.

(64) Tillmann, R.; Hallquist, M.; Jonsson, Å. M.; Kiendler-Scharr, A.; Saathoff, H.; Iinuma, Y.; Mentel, T. F. Influence of Relative Humidity and Temperature on the Production of Pinonaldehyde and OH Radicals from the Ozonolysis of Alpha-Pinene. *Atmos. Chem. Phys.* **2010**, *10*, 7057–7072.

(65) Ryzhkov, A. B.; Ariya, P. A. The Importance of Water Clusters (H₂O)_n (n = 2, ..., 4) in the Reaction of Criegee Intermediate with Water in the Atmosphere. *Chem. Phys. Lett.* **2006**, *419*, 479–485.

(66) Lee, J. D.; Lewis, A. C.; Monks, P. S.; Jacob, M.; Hamilton, J. F.; Hopkins, J. R.; Watson, N. M.; Saxton, J. E.; Ennis, C.; Carpenter, L. J.; et al. Ozone Photochemistry and Elevated Isoprene during the UK Heatwave of August 2003. *Atmos. Environ.* **2006**, *40*, 7598–7613.

(67) Ren, X.; Harder, H.; Martinez, M.; Leshner, R. L.; Oligier, A.; Simpas, J. B.; Brune, W. H.; Schwab, J. J.; Demerjian, K. L.; He, Y.; et al. OH and HO₂ Chemistry in the Urban Atmosphere of New York City. *Atmos. Environ.* **2003**, *37*, 3639–3651.

(68) Atkinson, R.; Aschmann, S. M. OH Radical Production from the Gas-Phase Reactions of O₃ with a Series of Alkenes under Atmospheric Conditions. *Environ. Sci. Technol.* **1993**, *27*, 1357–1363.

(69) Neeb, P.; Moortgat, G. K. Formation of OH Radicals in the Gas-Phase Reaction of Propene, Isobutene, and Isoprene with O₃: Yields and Mechanistic Implications. *J. Phys. Chem. A* **1999**, *103*, 9003–9012.

(70) Aschmann, S. M.; Tuazon, E. C.; Arey, J.; Atkinson, R. Products of the Gas-Phase Reaction of O₃ with Cyclohexene. *J. Phys. Chem. A* **2003**, *107*, 2247–2255.

(71) Horie, O.; Neep, P.; Moortgat, G. K. Ozonolysis of *trans*-2-Butenes and *cis*-2-Butenes in Low Parts-Per-Million Concentration Ranges. *Int. J. Chem. Kinet.* **1994**, *26*, 1075–1094.

(72) McGill, D. D.; Rickard, A. R.; Johnson, D.; Marston, G. Product Yields in the Reactions of Ozone with *Z*-but-2-ene, *E*-but-2-ene and 2-Methylbut-2-ene. *Chemosphere* **1999**, *38*, 1205–1212.

(73) Orzechowska, G. E.; Paulson, S. E. Production of OH Radicals from the Reactions of C4–C6 Internal Alkenes and Styrenes with Ozone in the Gas Phase. *Atmos. Environ.* **2002**, *36*, 571–581.

(74) Hasson, A. S.; Chung, M. Y.; Kuwata, K. T.; Converse, A. D.; Krohn, D.; Paulson, S. E. Reaction of Criegee Intermediates with Water Vapor: An Additional Source of OH Radicals in Alkene Ozonolysis? *J. Phys. Chem. A* **2003**, *107*, 6176–6182.